

**Viscosity/Elasticity****Determination of the First and Second Normal Stress Differences in the Truncated-Cone-and-Plate Apparatus****1. Measurements on a Polyisobutylene/Decalin Solution****G. A. Alvarez<sup>1,2</sup>, A. S. Lodge<sup>2</sup> and H.-J. Cantow<sup>1</sup>**<sup>1</sup> Institut für Makromolekulare Chemie der Universität Freiburg, Hermann-Staudinger-Haus, Stefan-Meier-Strasse 31, D-7800 Freiburg i. Br., Federal Republic of Germany<sup>2</sup> Rheology Reserach Center, University of Wisconsin-Madison, 1500 Johnson Drive, Madison, WI 53706, USA**SUMMARY**

The steady state radial pressure distribution in the truncated cone-and-plate (TCP) apparatus has been measured for a highly elastic polyisobutylene solution in cis-trans decalin ( $M_w = 4300 \text{ kgmol}^{-1}$ ,  $M_w/M_n = 2$ ) at eight shear rates from 1 to  $270 \text{ s}^{-1}$  and temperatures of 3.0, 20.0, 30.0 and  $46.0^\circ\text{C}$ . The slope of pressure, corrected for inertia by the classical formula, versus the logarithm of radius provides a combination of normal stress differences  $N_1 + 2N_2$  with a typical experimental scatter of 1 % at all measured temperatures and shear rates. The plots of  $N_1 + 2N_2$  versus shear rate can be shifted, without loss of accuracy, by means of the time-temperature superposition principle, the shift factors strictly adhering to a WLF equation. Extrapolated rim pressures, when corrected for elastic hole pressure with a theoretical equation, give values of the second normal stress difference with typically less than 10 % of experimental scatter. Contrary to previous analyses of the TCP apparatus, the center-hole pressure is found to give a useful estimate of the second normal stress difference, although there are insufficient data at present to perform the differentiation of a nonlinear function required in the analysis of the data. Instrument imperfections are reviewed briefly in the Appendix.

**INTRODUCTION**

There is currently a new interest in the study of normal stress differences in polymers. Theoretically, CURTISS and BIRD have extended their kinetic theory calculations to polymer melts <sup>1</sup> and rigid rod-like polymers in solution <sup>2</sup> with new results about the effect of molecular structure on the second normal stress difference. Experimentally, a truncated cone-and-plate (TCP) apparatus has been constructed and tested by LODGE and HOU <sup>3</sup>, which is also investigating the hole pressure <sup>4</sup> inherent in some of the data analyses for the TPC apparatus. Computer methods are also being applied in the study of the hole pressure <sup>5</sup>.

The measurement of the radial pressure distribution in the cone-and-plate (or parallel plate) rheometer is the only known method to give both first and normal stress differences from a single experiment. A combination of normal stress differences  $N_1 + 2N_2$  is obtained from the slope of pressure versus the logarithm of the radius, and the extrapolated rim pressure gives, in the absence of hole pressure, the second normal stress difference. An additional combination of normal stress differences  $N_1 + N_2$  can be derived from measurement of pressure at the center of the plate in the TCP apparatus. We report here normal stress differences for a high-molecular-weight polyisobutylene solution in the TCP apparatus, which are more accurate and extend over a larger temperature and shear-rate range than previously achieved. Samples of the same polyisobutylene solution as reported here have been distributed

by Professor K. WALTERS, University College, Wales, to Professor R. I. TANNER, University of Sidney, Australia, and Professor E. B. CHRISTIANSEN, University of Utah, in order to encompass a wide variety of experimental techniques for measuring normal stress differences. Results of this joint measurement project will be compared in the near future with the aim of establishing standard values of normal stress differences on a given liquid, as well as of reviewing the experimental techniques available at present for measuring normal stress differences in polymeric liquids.

## THEORY

Under certain assumptions about the liquid in the cone-and-plate gap and the state of flow, integration of the  $r$ -component of the stress equations of motion gives the result <sup>6</sup>

$$p(r, \Omega) = p(R, \Omega) - (N_1 + 2N_2) \ln\left(\frac{r}{R}\right) + p_p \quad (1) \quad \text{and} \quad p(R, \Omega) = -N_2 - p^* \quad (2)$$

where  $p(r, \Omega)$  is the pressure measured on the plate at radius  $r$ , for a cone angular velocity  $\Omega$ ,  $R$  is the plate radius,  $N_1$  and  $N_2$  are the first and second normal stress differences, and  $p_p$  is the pressure due to inertial forces.  $p^*$  is the hole pressure which arises due to the use of holes leading to chambers where pressure is measured by large diaphragm transducers. The shear rate is  $\dot{\gamma} = \Omega/\alpha$ , where  $\alpha$  is the cone angle.

It has usually been assumed that the inertial pressure  $p_p$  for a viscoelastic liquid is the same as that for a Newtonian liquid, and is given by:

$$p_p = 0.15\rho\Omega^2(r^2 - R^2) \quad (3)$$

where  $\rho$  is the liquid density. This assumption is valid for low- and high-elasticity liquids, when judged by its ability to generate the viscoelastic pressure distribution of equation (1) <sup>3</sup>.

Secondary flow, which has the velocity components other than tangential, affects the validity of the equations above. Viscoelastic pressure due to secondary flow should be very small at all usable shear rates and cone angles, according to perturbation calculations and measurements with different cone angles <sup>3, 7</sup>. Viscoelastic perturbations to the hole pressure are also implicitly neglected. However, inertial pressures are much more sensitive to secondary flow, and both  $p_p$  and  $p^*$  are affected. The perturbation of inertial pressures due to secondary flow in Newtonian liquids is the subject of current research and will be presented elsewhere. In summary, as a generalization for equation (3), the inertial contribution becomes

$$p_p = A(\text{Re})\rho\Omega^2[(r^2 - R^2) + B(\text{Re})(r^2 - R^2)^2 + \dots] \quad (4)$$

where  $\text{Re} = \Omega R^2/\nu$  is the Reynolds number,  $\nu$  is the kinematic viscosity, and  $A$ ,  $B$ , etc., are functions to be determined experimentally. Similarly, a Newtonian hole pressure  $p_p^*$  appears as a result of secondary flow, but is zero otherwise. Further assumptions would be required to introduce the corresponding corrections for viscoelastic liquids.

Secondary flow has not been taken into account in the analysis given below, where inertia is at most 10% of the measured pressure. It is possible that accuracy could be improved by making secondary flow corrections.

Viscosity measurements are essential in order to apply equation (4) to the present data. Furthermore, the concept of the equivalent Newtonian liquid, i. e., a liquid with the same density and viscosity as the viscoelastic liquid, has not yet been tested in the cone- and -plate apparatus, although the same idea appears to be successful in the data handling of the Newtonian hole pressure <sup>4</sup>.

Measurement of the pressure  $p_0$  at the center of the plate gives <sup>8</sup>

$$N_1 + N_2 = \dot{\gamma} \frac{d}{d\dot{\gamma}} [p_0 - (N_1 + 2N_2) \ln(\frac{R}{r_0})] \quad (5)$$

where  $r_0$  is the radius of the truncated cone apex. The final result,  $N_1 + N_2$ , will contain errors in  $p_0$  and  $N_1 + N_2$ , and some means must be found to perform the differentiation with respect to shear rate.

Finally, a theoretical equation relates hole pressure for circular holes to a combination of normal stress differences as follows <sup>4</sup>:

$$N_1 - N_2 = 3p^* e \frac{d \ln p^*}{d \ln \sigma} \quad (6)$$

where  $\sigma$  is the shear stress, and  $p^* = p^* - p_p$ .

## EXPERIMENTAL

A 2 % w/v solution of polyisobutylene ( $M_w = 4300 \text{ kg mol}^{-1}$ ,  $M_w/M_n = 2$ ) in a mixture of cis and trans decalin (sample "D1", dated January 1983) was received from Professor K. WALTERS, Wales. Measurements at 20<sup>o</sup> C were made on February 17, 1983, and on February 23, 1983, as shown in Table 1. Measurements at 3.0, 30.0 and 46.0<sup>o</sup> C were made between these dates. The apparatus and operating procedure have been carefully described elsewhere <sup>3</sup>. The only additions were thermal

**Table 1:** Comparison of slopes and intercepts of radial pressure distributions in TCP apparatus for measurements at 20<sup>o</sup> C on 17 February 1983 (first run) and 23 February 1983 (last run).

Shear rate [s <sup>-1</sup> ]	- 1 x slope = $N_1 + 2N_2$ [Pa]			- 1 x intercept = $N_2 + p^*$ [Pa]			Correlation coefficient	
	First run	Last run	% change	First run	Last run	% change	First run	Last run
1.071	11.7	--	--	0.52	--	--	0.99	--
3.385	30.9	30.2	2.1	2.2	1.8	19	0.994	0.992
10.712	69.9	68.9	1.4	6.0	4.7	29	0.9995	0.9994
27.006	128	127	1.0	11.7	11.2	4.9	0.9997	0.9998
53.922	213	212	0.4	22.0	22.8	3.7	0.9999	0.9999
107.10	386	379	2.0	48.9	46.0	6.3	1.0000	0.9999
214.48	752	742	1.3	97.9	97.6	0.3	1.0000	0.9997
269.79	--	936	--	--	117	--	--	0.9998

insulation of all thermostated parts and a vapor shield consisting of a stainless steel ring sitting on the plate and enclosing the vertical wall of the cone of height 15 mm, with an air gap between the rotating cone and the stationary ring of 0.1 mm. This prevented evaporation of liquid and helped towards temperature homogeneity in the gap. Temperature control was achieved by means of thermostated water, which was pumped separately to the cone, the plate, and the cone shaft. Temperatures were measured with an electronic thermometer calibrated against a certified glass thermometer. All temperatures were accurate and steady to  $\pm 0.03^{\circ}$  C. The density of the solution at 20<sup>o</sup> C was 884 kg mol<sup>-1</sup>, and the thermal expansion coefficient in the range from 3.0 to 46.0<sup>o</sup> C was  $8.56 \times 10^{-4} \text{ }^{\circ}\text{C}^{-1}$ ; both values were measured by dilatometry.

Pressures were measured by means of hole-mounted diaphragm capacitance transducers by the following procedure: (1) after the gap was filled with liquid at the run temperature, the transducer diaphragms were restored approximately to their undeflected position by a counter-pressure of air and zeroed electronically; (2) with the motor off, the electronic baseline was read for each transducer on a chart recorder; (3) with the motor in steady rotation and after pressure equilibration, the transducer diaphragms were restored to their static position by means of a counterpressure of air, monitored by the return of the electronic signals on the chart recorder to the static baselines.

The counterpressure of air was measured on a micromanometer, Steps 2 and 3 were repeated for each angular velocity, once in the forward and once in the reverse direction. The reason for recording both senses of rotation is given in the Appendix.

The filling of the gap with liquid was done as before by forcing the liquid slowly from a reservoir, through the bottom of the transducers, into the gap, by air pressure, but the original glass tubing and manifold were replaced by 2-mm-diameter stainless-steel tubing, reducing the volume of liquid trapped in the tubing outside the gap from 40 cc to 10 cc. The volume of liquid required to fill the gap was 30 cc for the  $3^\circ$  cone angle. It was possible, with some practice, to fill the gap reproducibly to a point where the liquid would burst out of the gap if the plate were raised by  $10\ \mu\text{m}$ . It was not possible, as explained in the Appendix, to study the shape of the gap in the dynamic state.

## RESULTS AND DISCUSSION

Viscoelastic pressure, defined as measured pressure minus the inertial correction from equation (3), is plotted in Fig. 1 versus the logarithm of the radius for the first and last run with the polyisobutylene solution, both at  $20.0^\circ\text{C}$ . Each pressure is measured twice, once in the forward and once in the reverse direction, and the best straight line is drawn through the average of both senses of rotation by a least squares fit. The slopes and intercepts of these graphs are shown in Table I.

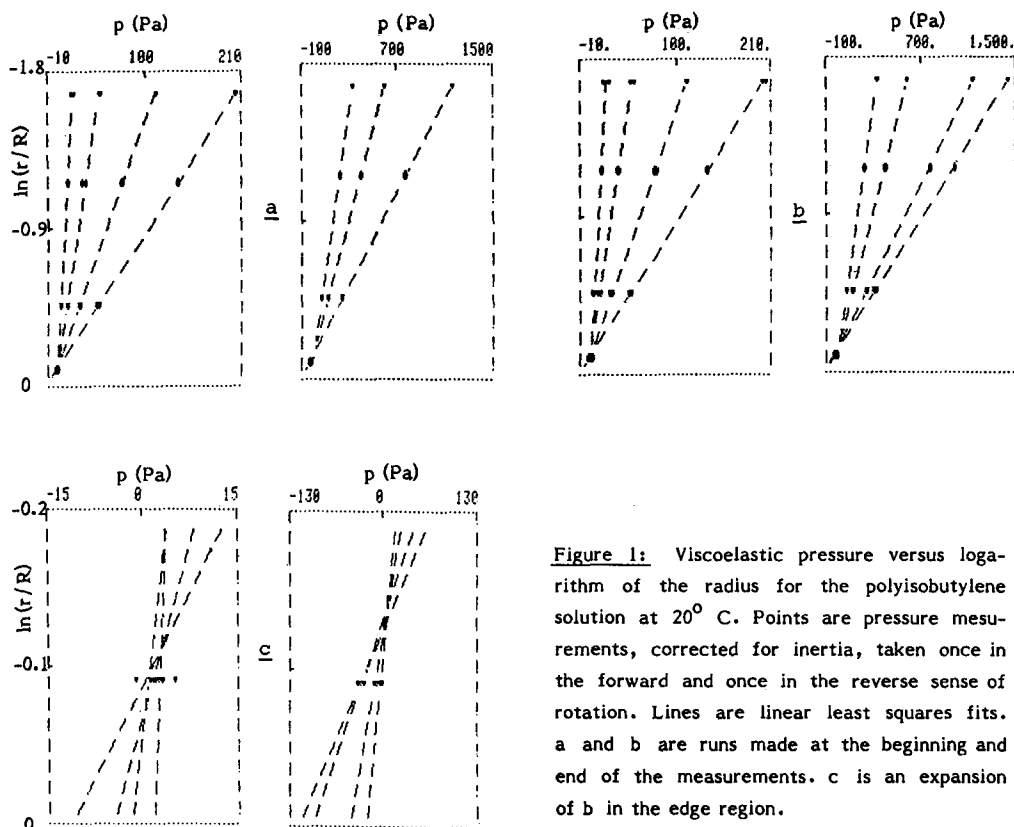


**Figure 1:** Viscoelastic pressure versus logarithm of the radius for the polyisobutylene solution at  $20^\circ\text{C}$ . Points are pressure measurements, corrected for inertia, taken once in the forward and once in the reverse sense of rotation. Lines are linear least squares fits. a and b are runs made at the beginning and end of the measurements. c is an expansion of b in the edge region.

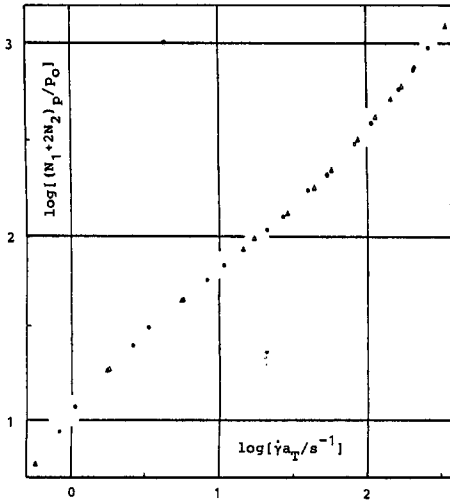


**Figure 2:** Slopes of plots as in Fig. 1, which give  $N_1 + 2N_2$  for measurements at temperatures:  $\blacktriangle$   $3.0^\circ\text{C}$ ,  $\bullet$   $20.0^\circ\text{C}$ ,  $\circ$   $30.0^\circ\text{C}$ ,  $\Delta$   $46.0^\circ\text{C}$ , reduced by time - temperature superposition. Reference temperature:  $20^\circ\text{C}$ .

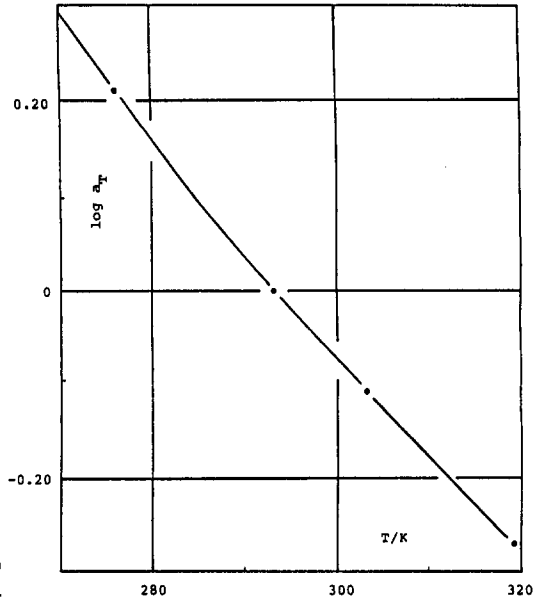


**Figure 3:** Shift factors required to reduce data from Fig. 2, versus temperature. Line is given by WLF equation  $c_1^0 = 2.79$  and  $c_2^0 = 243.3$ .

Measurements at  $3.0$ ,  $30.0$ , and  $46.0^\circ\text{C}$  are similar to those of Fig. 1. The very good quality of the straight lines obtained in all the measurements attests to the degree of confidence which can be given to some of the assumptions about the experiment, in particular the inertial correction given by (3). The negative slopes from Fig. 1, which according to equation (1) give  $N_1 + 2N_2$ , are plotted in Fig. 2 versus shear rate, for the temperatures employed of  $3.0$ ,  $20.0$ ,  $30.0$ , and  $46.0^\circ\text{C}$ . The ordinate has been reduced in temperature and density according to

$$(N_1 + 2N_2)_p = \frac{T_0}{T} \left(\frac{\rho_0}{\rho}\right)^2 (N_1 + 2N_2) \tag{7}$$

and the abscissas are shifted along the shear - rate scale to achieve superposition on the curve at the reference temperature of  $293.2\text{K}$ . The shift factors are plotted in Fig. 3 versus temperature, where the solid line is given by the WILLIAMS - LANDEL - FERRY equation <sup>9</sup>:

$$\log a_T = \frac{-c_1^0 (T - T_0)}{c_2^0 + T - T_0} \tag{8}$$

This procedure, known as time - temperature superposition, which is usually applied to the storage modulus  $G'$  because of its origin in the frequency dependence of the glass transition temperature, is partially justified in view of the exact relationship <sup>6</sup>

$$\lim_{\omega \rightarrow 0} \frac{G'}{\omega^2} = \lim_{\dot{\gamma} \rightarrow 0} \frac{1}{2} \frac{N_1}{\dot{\gamma}^2} \tag{9}$$

and the excellent degree to which the nontrivial line shapes are matched in Fig. 2 for each temperature. The values of  $c_1^0 = 2.8$  and  $c_2^0 = 243.3$  obtained from Fig. 3 are in reasonable agreement with the values of  $c_1^0 = 8.4$  and  $c_2^0 = 200.4$  quoted for isobutylene in the standard reference<sup>9</sup>. These values, being free volume parameters, are, however, extremely sensitive to molecular structure, molecular weight, etc.

The second normal stress difference obtained from the intercepts in Fig. 1, according to equation (2), with  $p^*$  calculated from equation (6) assuming  $d \ln p^*/d \ln \sigma = 1.88$ , and  $N_1 + 2N_2$  from Fig. 2, is presented in Fig. 4. Given the effective shear rate of 0.5 to 350  $s^{-1}$  and the consistency of the measurements at all temperatures as seen in the reduced plot, we believe this is the most extensive and accurate measurement of the second normal stress difference reported to date. The value  $d \ln p^*/d \ln \sigma = 1.88$  was obtained by P. P. TONG (Ph. D. dissertation, University of Wisconsin - Madison, 1980) for a similar solution consisting of 2.3 wt. % of polyisobutylene (B 200) in Exxon Primol. We have used this as an interim value until we have made our own measurement of this equation.

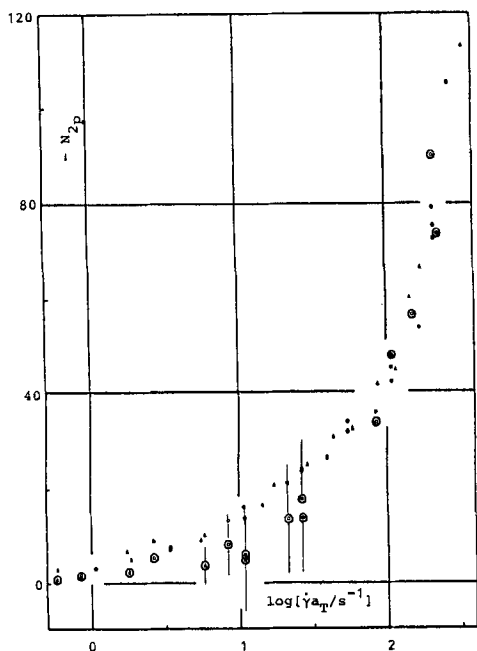


**Figure 4:** Second normal stress difference obtained from intercepts of Fig. 1 and theoretical equation (6) for hole pressure; temperature and shift factors are the same as in Fig. 2. Points enclosed by a circle were obtained from equation (5).

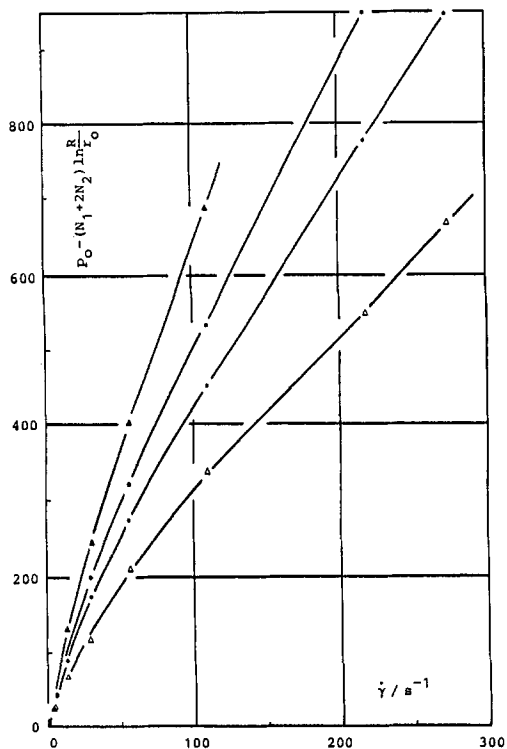


**Figure 5:** Plot of the function  $P_0 - (N_1 + 2N_2) \ln \frac{R}{R_0}$  against shear rate. The slopes of this plot give  $(N_1 + N_2)$ . Temperatures as in Fig. 2. Lines are smoothed functions through the data.

The TCP apparatus provides also  $N_1 + N_2$  from the pressure at the center of the plate, after differentiating the function  $p_0 - (N_1 + N_2) \ln \frac{R}{R_0}$  with respect to shear rate. This function is plotted in Fig. 5. Values of  $N_2$  from the slopes of the smoothed functions are, over a good part of the range, in good agreement with those in Fig. 4; at intermediate shear rates, more points than presently available are required due to the rapid change of slope in this region. Important tests of equation (6) could be made from this method, although additional scatter from  $p_0$  as well as  $N_1 + 2N_2$  will be present in Fig. 5. The opposite conclusion reached by LODGE and HOU<sup>3</sup> is probably due to their use of a less elastic solution than presently employed. Alternatively, the total thrust under the truncated cone would give directly another combination of normal stress differences without differentiation of the data. Such an idea is under consideration in future developments of the TCP apparatus.

### CONCLUSIONS

1. The slopes of lines representing viscoelastic pressure versus log radius can be measured in the temperature range 3 to 46° C and shear rate 1 to 270 s<sup>-1</sup> within a scatter of 1 % for a viscoelastic fluid.
2. The time - temperature superposition principle can be applied to normal stress differences as judged by accurate matching of the nontrivial line shapes and strict adherence to a WLF equation.
3. The second normal stress difference obtained from extrapolation to rim pressure can be measured with a scatter of less than 10 % in a shear - rate range of 0.5 to 350 s<sup>-1</sup>.
4. Assumptions about inertia, secondary flow, boundary conditions, etc., appear to be correct over the temperature and shear - rate ranges studied.
5. Provided a large number of measurements were made for accurate determination of the slope of a nonlinear function, important conclusions about hole pressure in the TCP apparatus could be reached.
6. Viscosity and, hopefully, zero - shear viscosity, as well as molecular weight and concentration effects, should be studied in order to obtain molecular parameters to test models.
7. Certain instrument imperfections mentioned in the Appendix require attention before more accurate measurements can be attempted and the shape of the free boundary be photographed and analyzed.

### ACKNOWLEDGMENTS

G. A. A. and H. - J. C. gratefully acknowledge financial support from the DEUTSCHE FORSCHUNGSGEMEINSCHAFT and the RHEOLOGY RESEARCH CENTER OF THE UNIVERSITY OF WISCONSIN.

### APPENDIX

The following instrument imperfections are known to affect the quality of the data from the TCP apparatus:

1. It is well known, since the pioneering studies of ADAMS and LODGE<sup>7</sup>, that alignment of the plate with respect to the cone axis must be achieved to a high degree of perfection in order to avoid converging and diverging fields on the plate that generate large pressures which change sign

with the sense of rotation. Alignment is greatly facilitated in the TCP apparatus by a kinematic mounting of the plate which consists of loading the plate by three stiff springs against three pins adjusted in height so that a constant gap between a capacitance transducer mounted at the edge of and rotating with the cone, and the plate can be as nearly as possible realized. The measured gap between the transducer and the plate is given in Fig. A 1, where the presence of a 4- $\mu\text{m}$  furrow is clearly seen. Further lapping of the plate is required to remove this imperfection in order to achieve optimum alignment; this is especially important at lower viscosity, possibly due to the time constant of the liquid being sufficiently small to accommodate rapid change in the flow conditions.

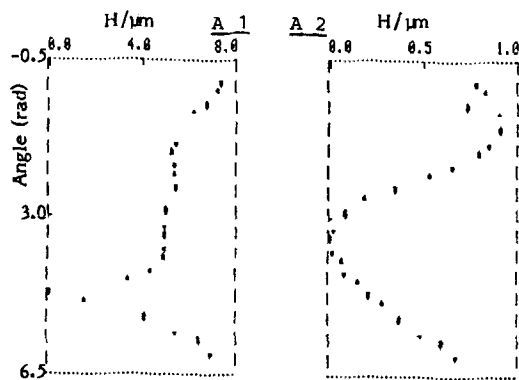


Figure A 1: Plate level map obtained with capacitance transducer mounted at the edge of the cone and rotating with it. Curvature is due to alignment, but position and depth of furrow are independent of alignment.

Figure A 2: Axial bearing movement monitored by capacitance transducer placed at the center of the plate with cone apex as second electrode.

2. By placing the capacitance gauge at the center of the plate, with the cone truncation as a second electrode, the axial movement of the cone can be detected, as shown in Fig. A 2. This effect imposes oscillations in the baseline of the measurements and is currently studied quantitatively.
3. A lateral motion of the liquid in the gap, which increases with shear rate and eventually limits the shear rate attainable, is believed to be due to an eccentricity of the cone outer surface with respect to its axis. Work is in progress to remove this defect by machining in situ the vertical wall of the cone.

## REFERENCES

1. CURTISS, C. F. and BIRD, R. B., *J. Chem. Phys.* **74**, 2016, 2026 (1981)
2. BIRD, R. B. and CURTISS, C. F., University of Wisconsin Rheology Research Center Report No. 84, March 1983
3. LODGE, A. S. and HOU, T. H., *Rheol. Acta* **20**, 247 (1981)
4. LODGE, A. S., *Hole Pressure and Normal Stress Differences*, Polymer News, 1983
5. JACKSON, N. R. and FINLAYSON, B. A., *J. Non-Newtonian Fluid Mech.* **10**, 71 (1982)
6. LODGE, A. S., *Body Tensor Fields in Continuum Mechanics*, Academic Press, 1974
7. ADAMS, N. A. and LODGE, A. S., *Phil. Trans. A* **256**, 149 (1964)
8. LODGE, A. S., *Rheol. Acta* **10**, 554 (1971)
9. FERRY, J. D., *Viscoelastic Properties of Polymers*, Wiley, 1982